Selective growth of nanometer-scale Ga dots on Si(111) surface windows formed in an ultrathin SiO_2 film

Motoshi Shibata
Joint Research Center for Atom Technology, Angstrom Technology Partnership, c/o National Institute for Advanced Interdisciplinary Research, 1-1-4 Higashi, Tsukuba, Ibaraki 305-0046, Japan

Stoyan S. Stoyanov*
Joint Research Center for Atom Technology, National Institute for Advanced Interdisciplinary Research, 1-1-4 Higashi, Tsukuba, Ibaraki 305-0046, Japan

Masakazu Ichikawa
Joint Research Center for Atom Technology, Angstrom Technology Partnership, c/o National Institute for Advanced Interdisciplinary Research, 1-1-4 Higashi, Tsukuba, Ibaraki 305-0046, Japan
(Received 21 October 1998)

Selective growth of nanometer-scale Ga dots on patterned ultrathin SiO_2 films was studied by using scanning-reflection electron microscopy and energy-dispersive x-ray spectroscopy (EDX). Nanometer-scale Si(111) surface windows were fabricated by electron-beam-induced thermal decomposition of the film. Ga was deposited on the patterned surfaces at room temperature to 550 °C. Under certain deposition and annealing conditions, Ga dots were present only on the Si(111) surface windows, and the smallest size of the dots was about 20 nm. To understand the selective growth of Ga dots, we measured the desorption rate and the surface-diffusion length of Ga atoms until all atoms desorbed from the SiO_2 surface and nucleated forming random dots. The EDX measurement showed that the desorption rate from Ga dots on SiO_2 films was 2 to 2.5 times larger than that on Si(111) surfaces, and that the activation energy of desorption rate from SiO_2 films was 1.33 eV. The Ga surface-diffusion length was estimated by measuring the temperature dependence of the Ga depleted zone width near the linear Si surface windows. The surface-diffusion length of Ga atoms on ultrathin SiO_2 films increased when the substrate temperature was increased. Thus, we were able to selectively grow Ga dots on only the Si(111) surface windows. [S0163-1829(99)02716-2]

I. INTRODUCTION

Selective growth is an important technique in large-scale integrated circuit technology and nanofabrication, especially on patterned silicon dioxide (SiO_2) film. Here we call an SiO_2 area a mask, and an exposed semiconductor area, a window. Although selective growth of Si (Ref. 1) and GaAs (Refs. 2–6) have been studied using chemical beam epitaxy and metal-organic chemical-vapor deposition with gaseous sources, a recent study by Allegetti and Nishinaga[7] reported on the selective growth of GaAs using Ga and As_4 as source materials. In their growth experiment, the molecular beam of Ga was periodically supplied under the constant pressure of As_4 at a substrate temperature of 630 °C. During the interruption, GaAs polycrystals grown on the mask area were decomposed into Ga and As atoms, and these atoms on the mask were desorbed or diffused to window areas. Since, in their experiment, the pressure of As_4 over the surface was kept constant, we consider that the desorption and diffusion of Ga atoms on the mask play an important role for this selective-growth process. Although the diffusion of Ga atoms on GaAs surfaces has been reported,[8,9] little is known about the diffusion and desorption of Ga atom on SiO_2 films. Since the roughness of SiO_2 film influences the desorption and diffusion, we consider that a study of them requires well-defined SiO_2 films.

Recently, an ultrathin SiO_2 film with a thickness less than 1 nm on Si(111) surfaces received considerable attention. Previous x-ray photoelectron spectroscopy and scanning tunneling microscopy studies reported that the oxide film is composed of SiO_2,[10] and that atomic steps can clearly be seen.[11,12] Their experimental results indicated that SiO_2 films on Si(111) surfaces are of good quality and the SiO_2 film has very little roughness. A patterning process on ultrathin SiO_2 films using scanning-reflection electron microscopy (SREM) have been reported by Fujita *et al.*;[13] line-shaped windows of 10 nm in width were fabricated under ultrahigh vacuum (UHV) conditions. In the electron-beam irradiated area in the SiO_2 film, the composition of SiO_2 changes to SiO due to electron-stimulated desorption; oxygen desorbs from SiO_2 films.[14] During annealing, the SiO in the film is easily volatilized, and the window areas are then exposed in the SiO_2 film. Applying molecular beam epitaxy (MBE) technique, Si and Ge nanostructures were formed on the patterned window area.[13,15] The roughness of the ultrathin SiO_2 film is very small. Moreover, patterning and deposition can be performed under UHV conditions. Hence, we consider ultrathin SiO_2 films to be suitable for studies on the desorption and diffusion of Ga atoms.

On the other hand, a recent study by Chikyo and Koguchi[16] reported GaAs dots of 45-nm in diameter on the Se-terminated GaAs surface. In their experiment, self-

organized Ga dots were formed on the Se-terminated GaAs surface by using an MBE technique. The Ga dots were then allowed to react with As. Because the position of Ga dots is accidentally determined, it is difficult to control. Applying the nanofabrication technique reported by Fujita *et al.*,[13] we can expect that the nanometer-scale Ga dots on the Si(111) surface window will be selectively grown on Si(111) surfaces and that well-ordered quantum dots of GaAs or GaN will be formed when Ga dots are allowed to react with As or N.

In this paper, we determine conditions needed to form only Ga dots on the Si(111) surface windows, and we compare the Ga dots on Si(111) surface windows with those on ultrathin SiO_2 films. Moreover, we study the desorption and diffusion of Ga atoms on SiO_2 films in order to understand the mechanism of the selective growth of Ga dots.

II. EXPERIMENT

The apparatus consists of a load-lock, an UHV preparation, and an UHV main chambers. Sample can be transferred from one chamber to another one without breaking UHV. The main chamber is equipped with SREM, MBE, and an energy-dispersive x-ray (EDX) spectrometer. In the main chamber, sample cleaning, SREM observation, window fabrication, Ga deposition, annealing, and EDX measurement are performed. Oxidation is performed in the preparation chamber. Details of the apparatus have been described elsewhere.[17]

Well-oriented *n*-type Si(111) wafers were used in this study. To remove native oxide layers on the sample, thermal treatment was done as follows: the sample was heated to 600 °C by passing a direct current through the sample, and then kept in an UHV condition for several hours. After that, it was flashed several times at 1200 °C below 4×10^{-8} Pa. Finally, the clean surface was examined with microprobe reflection high-energy electron diffraction (μ-RHEED) and SREM. Thermal oxidation was done in molecular oxygen at a pressure of 1.33×10^{-2} Pa at 720 °C for 2 min. The film thickness was estimated to be 0.5 nm.[10] The fabrication of Si(111) surface windows in the SiO_2 film was done according to the sequence reported by Fujita *et al.*;[13] the surface was irradiated by using a focused electron beam used in SREM at a room temperature (RT) and subsequent annealing at 730 °C for a few minutes. Using a pyrolytic boron nitride (PBN) Knudsen cell, we deposited Gallium onto the surface at RT to 570 °C. The deposition rate was about 0.19 ML/min. The annealing process was done at 450–620 °C. The desorption rates of Ga from Si(111) surfaces and SiO_2 films were measured using EDX spectroscopy.

In this paper, all the SREM images were compressed in the electron-beam incident direction (vertical direction) since the glancing angle of the electron beam to the sample surface was set to 2.3° in order to obtain a μ-RHEED pattern. The unit length in the vertical direction was about 24 times larger than that in the horizontal direction. To reduce the image compression, we often used a tilt compensation method, where the magnification of images in the vertical direction (parallel to the direction of the electron beam) was three times larger than the magnification of those in the horizontal direction. Then, the vertical-to-horizontal ratio of the images decreased 8:1. These ratios were changed depending on whether we used the tilt compensation method or not. Hence, the vertical and horizontal scale markers indicated by two different distances were shown as insets.

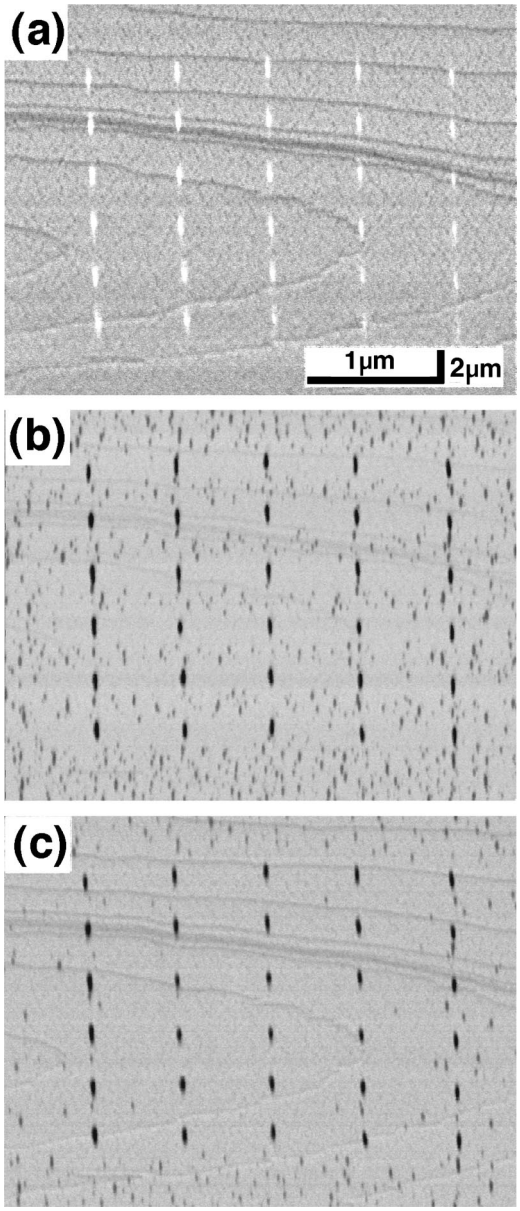

FIG. 1. Sequential SREM images of fabrication and selective-growth process. (a) after Si(111) surface windows fabrication, (b) annealing at 550 °C for 3 min after the deposition of 1 ML Ga at RT, and (c) additional annealing for 2 min after (b). All images have the same scale.

III. RESULTS AND DISCUSSION

A. Ga dots on Si(111) surface windows in SiO_2 films

Figure 1 shows the sequential SREM images of the fabrication and selective-growth processes. Ga of 1 ML was deposited on the surface, which was subsequently annealed at 550 °C for a few minutes. Figure 1(a) shows an SREM image of the surface after fabrication of the Si(111) surface windows. In this figure, the dark contrast lines correspond to the atomic steps at the SiO_2/Si(111) interface reported in a

previous study.[10] On the other hand, the bright contrast points are Si(111) surface windows in a SiO_2 film since the specular reflection spot intensity from the clean Si areas is significantly higher than that from the surface regions covered with amorphous SiO_2 films. Each window is 50 nm in the horizontal direction. In the horizontal direction, the distance between the windows is 0.65 μm and in the vertical direction 3 μm.

Figure 1(b) shows an SREM image of 1 ML Ga deposited at RT and annealed at 550 °C for 3 min. The dark and bright contrast areas correspond to Ga dots and SiO_2 film. Since the Ga dots intercept the electron beam, the contrasts of the window area are the reverse of those in Fig. 1(a). Well-ordered and random dots can be seen on the surface. The well-ordered dots are located on the Si(111) surface windows shown in Fig. 1(a). The size of the dots is nearly equal to the size of the windows. In contrast, the random dots of 20 nm in diameter are on the SiO_2 film. The size of the random dots is smaller than the size of the well-ordered dots. On this surface, we can find a so-called ''depleted zone,'' where the random dots cannot be seen. The existence of a depleted zone indicates that Ga atoms prefer to form dots on the window area rather than on the SiO_2 film. The width of a depleted zone d_z gives important information for the design of periodic windows for selective growth because random dots on SiO_2 films cannot be formed when the distance between the windows is smaller than $2d_z$. The depleted zones are observed between the well-ordered dots in the horizontal direction while that in the vertical direction are not clearly seen because the SREM image is compressed in the vertical direction. During the deposition at RT, Ga atoms on the SiO_2 film are uniformly distributed over the surface (not shown). Hence, during annealing, we consider that the Ga atoms diffuse to the window areas, desorb from the surface, and nucleate forming random dots.

Figure 1(c) shows an SREM image of additional annealing for 2 min after Fig. 1(b). In this image, the depleted zones are larger than those in Fig. 1(b), and are clearly observed around the well-ordered dots. Some of the random dots have disappeared while the well-ordered dots are preserved. These results strongly suggest that Ga atoms on SiO_2 films diffuse to the window areas and desorb from SiO_2 films easier than from Si(111) surface windows. Hence, the nanometer-scale Ga dots on Si(111) surface windows can be formed by further annealing. The difference in the desorption rate between SiO_2 films and Si(111) surfaces will be described later.

Figure 2 shows an SREM image of 0.56 ML Ga deposited at 550 °C. The arrangement of the dotted windows array is the same as that in Fig. 1(a). The dark and bright contrast areas correspond to Ga dots and SiO_2 film. We can see the well-ordered dots on the dotted windows but we cannot see the random dots on the SiO_2 film. This indicates that Ga dot nucleation hardly takes place on a SiO_2 surface under these deposition conditions. The smallest size of the dots is about 20 nm. The most important parameter determining the size of the dots is considered to be the thermal drift during the window fabrication since the electron-beam irradiation area becomes larger. For deposition above 560 °C, the Ga-induced 6.3×6.3 or $\sqrt{3} \times \sqrt{3}$ structure[18] is observed in the window areas, but Ga dots are not. In the course of this study, we found two processes in which Ga dots grow on the Si(111) surface windows only. For the first, Ga is deposited on the patterned surfaces at RT, and then the surface is annealed at 550 °C for more than 5 min. For the second, 0.56 ML of Ga is deposited at the surface temperature of 550 °C.

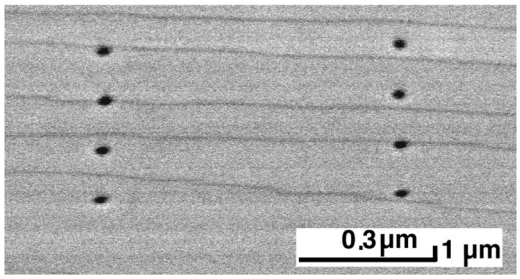

FIG. 2. An SREM image of 0.56 ML Ga deposited at 550 °C. Dark and bright contrast areas correspond to Ga dots and SiO_2 film. The tilt compensation method was not used.

B. Ga dots on SiO_2 films and Si(111) surfaces

Figure 3(a) shows a high-magnification SREM image of 1 ML Ga deposited at 510 °C on SiO_2 film. The dark and bright contrast areas correspond to Ga dots and SiO_2 film. Almost all the Ga dot images consist of a pair of circles. Since the glancing angle of an electron beam to the sample surface is set to 2.3°, the Ga dot intercepts the electron beam directly incident to the dot and the beam reflected from the surface neighboring the dot. The electron beam incidents from the lower to the upper side of the SREM image. There-

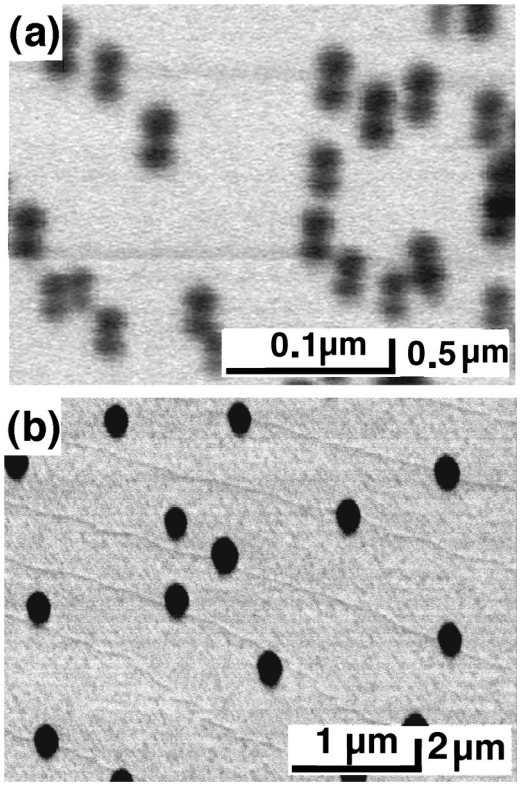

FIG. 3. (a) an SREM image of Ga dots on SiO_2 films after deposition of 1 ML Ga at 510 °C (the tilt compensation method was not used), and (b) an SREM image of Ga dots on a clean Si(111) surface after the deposition of 1.5 ML Ga at 510 °C.

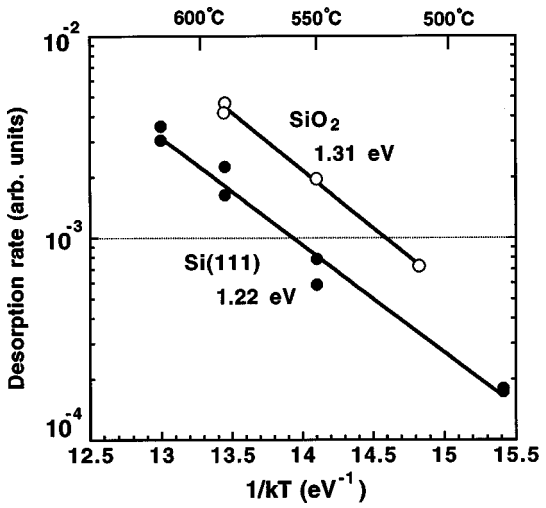

FIG. 4. Arrhenius plots of desorption rate on SiO_2 film and Si(111) surfaces. The measuring data on the SiO_2 film and Si(111) surface are indicated by the open and filled circles, respectively.

fore, the upper and lower part of the circles are, respectively, the real and shadow images of the dots. This indicates that the contact angle of the dots on the SiO_2 film is greater than 90° and thus that the Ga dots are repelled from a SiO_2 film. Each dot is about 20 nm. The number density of a dot is about $1.3\times10^9\,\mathrm{cm}^{-2}$. It is important that the dark area in the SREM image is proportional to a product of the height of a dot and the width in the horizontal direction of the image. In contrast, Fig. 3(b) shows a SREM image of Ga dots on a clean Si(111) surface after the deposition of 1.5 ML Ga at 510 °C. The dark and bright contrast areas correspond to Ga dots and a Ga-wetting layer. The size of the dots is about 200 nm, and this is about ten times larger than those on the SiO_2 film. The number density of the dots is about $1\times10^7\ \mathrm{cm}^{-2}$. The SREM image of Ga dots does not have a waist, as shown in Fig. 3(a). This indicates that Ga-wetting layers do not repel Ga dots, and Ga dots are easily formed on Si(111) surface windows.

C. Desorption of Ga dots on SiO_2 films and Si(111) surfaces

The desorption rates of Ga dots on SiO_2 films and Si(111) surfaces were measured using EDX. To avoid desorption during the EDX measurement, the measurement was done in the following way: Ga was deposited on the surfaces at RT, the sample was heated to 480–620 °C for a few minutes, and the EDX measurement was done at RT. The amounts of Ga deposited on the SiO_2 film and Si(111) surface were 1.5 and 2 ML. Since the intensities of the Ga and Si peaks were proportional to the electron dose, the amount of Ga on the surface was determined by the ratio of Ga:Si peaks. Figure 4 shows Arrhenius plots of the desorption rate on SiO_2 films and Si(111) surfaces. The desorption rate of Ga on SiO_2 film is 2 to 2.5 times larger than that of Ga on a Si(111) surface. The activation energies of desorption on SiO_2 films and Si(111) surfaces are 1.33 and 1.22 eV. The desorption rates indicate that random dots on SiO_2 films are desorbed easier than well-ordered dots on Si(111) surfaces, and this difference explains well the selective growth of Ga dots on Si(111) windows as shown in Fig. 1.

A previous study[19] reported that the activation energy of evaporation from Ga liquid, H_v, is 2.56 eV. This value is larger than those of Ga dots on the SiO_2 film and the Si(111) surface. In our observation of SiO_2 films and Si(111) surfaces, Ga dots were uniformly distributed over the surfaces [Figs. 3(a) and (b)]. Hence, we consider that the difference in the activation energy is related to the temperature dependence of the surface-diffusion length λ until desorption of Ga atom detached from Ga dot. λ is $\sqrt{D_s\tau_e}$, where D_s is the surface-diffusion coefficient and τ_e is the mean-residence time of Ga on the surface. When the average distance d between two neighboring Ga dots is less than 2λ, the whole Si (or SiO_2) surface contributes to the desorption rate because Ga atoms migrate over the whole surface and eventually leave it by desorption. In the opposite case $d>2\lambda$ Ga adatoms can be found only in the areas of the radius λ around each Ga dot. That is why the desorption rate in this case depends on the number density of Ga dots ρ as well as on the average diffusion distance λ. Hence, the temperature dependence of the desorption rate is given by $\rho\lambda^2\exp(-H_v/kT)$. The surface-diffusion length λ is proportional to $\exp[(E_{des}-E_{sd})/2kT]$, where E_{des} and E_{sd} are the activation energy of desorption and surface diffusion. The ρ has a temperature dependence: $\exp[E_{num}/kT]$. Thus, the desorption rate is proportional to $\exp[-(H_v-E_{des}+E_{sd}-E_{num})/kT]$. Generally, E_{des} is larger than E_{sd}. In our experiment, E_{num} is a positive value since the ρ decreases when the substrate temperature is increased. Therefore, for $d>2\lambda$, the activation energies are smaller for desorption from dots than from Ga liquid H_v. In our experiment, we confirmed this condition by comparing the estimation of λ and the Ga dot density ρ. The difference between the activation energies of the desorption rate on SiO_2 films and Si(111) surfaces is very small even though the activation energies are sensitive to surface conditions. Since the values of E_{des} and E_{sd} for Si(111) surfaces and SiO_2 films are not yet certain, we consider that their difference $(E_{des}-E_{sd}+E_{num})$ for Si(111) surfaces to be nearly equal to that for SiO_2 films.

D. Diffusion of Ga atoms on SiO_2 films

As shown in Figs. 1 and 2, the width of the depleted zone d_z gives important information for design of periodic windows for selective growth. Figures 5(a), 5(b), and 5(c) show SREM images of Ga dots on SiO_2 films with linear Si(111) surface windows after the deposition of 0.5 ML Ga at 450 °C, 1.0 ML Ga at 530 °C, and 1.5 ML Ga at 550 °C. Linear windows in the SiO_2 film were fabricated by the same technique as shown in Fig. 1(a). The dark lines, dots, and bright contrast areas correspond to the Ga lines on the windows, Ga dots, and SiO_2 films. The depleted zones are observed at both sides of the linear windows. The widths of zone d_z in Figs. 5(a), 5(b), and 5(c) are about 0.19, 0.27, and 0.49 μm, respectively.

Increasing the substrate temperature decreases the number density of the dots while the width of the depleted zone d_z increases, and Ga atoms migrate on the SiO_2 film, and either leave the surface by desorption or join some of the Ga dots. Hence, we define the effective lifetime of Ga atoms τ_{eff}:

$$1/\tau_{eff}=1/\tau_{des}+1/\tau_{nucl}, \tag{1}$$

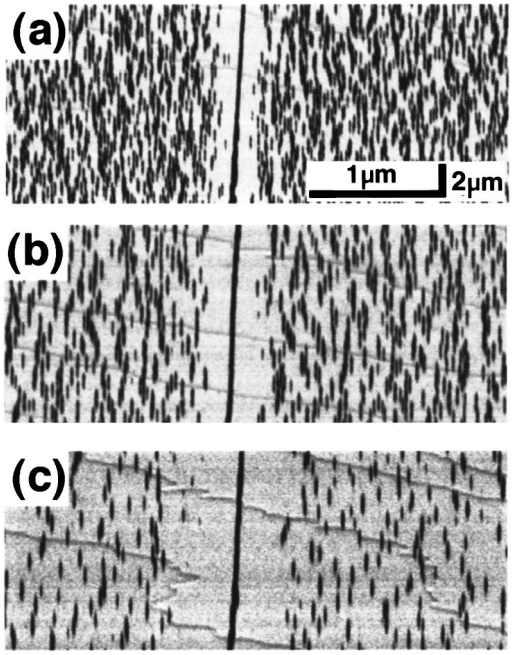

FIG. 5. SREM images of Ga dots on SiO_2 films with linear Si(111) surface windows after the deposition of Ga. (a) 0.5 ML at 450 °C, (b) 1.0 ML at 530 °C, and (c) 1.5 ML at 550 °C. The deposition rate is about 0.19 ML/min. All images have the same scale.

where τ_{des} and τ_{nucl} are the lifetime of a Ga atom in the state of mobile adsorption until it evaporates and attaches itself to Ga dots. Although $1/\tau_{nucl}$ has generally a position dependence (since the number density of Ga dots depends on the distance to the window), we assume that $1/\tau_{nucl}$ has no position dependence. The concentration of Ga atoms on the SiO_2 film as a function of distance to the linear window $n_s(x)$ is thus expressed by a one-dimensional diffusion equation:

$$\partial n_s(x)/\partial t = D_s \; d^2 n_s(x)/dx^2 - n_s(x)/\tau_{eff} + R_s = 0, \quad (2)$$

where the axis x is perpendicular to the linear window, D_s is the coefficient of surface diffusion, and R_s is the flux of Ga atoms arriving at SiO_2 films. The observation shown in Fig. 5 indicates that the linear window is quickly filled up with Ga. Hence, for $x=0$, the concentration $n_s(x)$ is equal to its equilibrium value n_s^e, where the two-dimensional gas of Ga atoms is in equilibrium with the liquid Ga covering the clean Si surface. Under this boundary condition, the concentration of Ga atoms on SiO_2 films $n_s(x)$ is given by:

$$n_s(x) = R_s\tau_{eff} + (n_s^e - R_s\tau_{eff})\exp(-x/\lambda_s), \quad (3)$$

where surface-diffusion length λ_s is defined as $\sqrt{D_s\tau_{eff}}$.

On the other hand, the number density of a Ga dot is expressed by $I_n(x)t_d$, where $I_n(x)$ and t_d are the rate of Ga-dot nucleation and deposition time. When the Ga dot is assumed to have the spherical shapes shown in Fig. 3(a), $I_n(x)$ is given by:[20]

$$I_n(x) = N_0\omega(x)\exp[-\Delta G(x)/kT], \quad (4)$$

$$\omega(x) = D_s n_s(x), \quad (5)$$

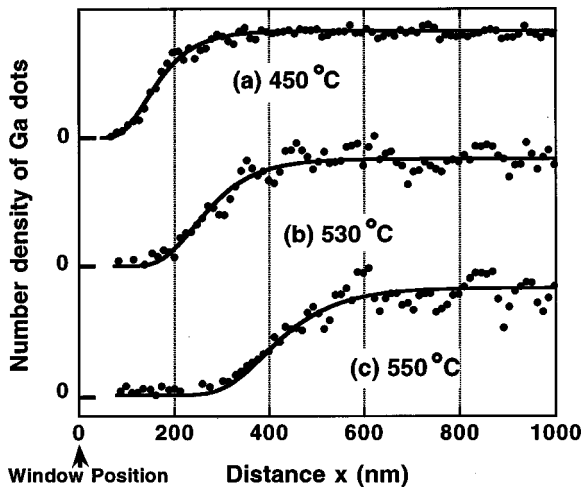

FIG. 6. Number density of Ga dots as a function of distance from linear windows in horizontal direction. (a) 450 °C, (b) 530 °C, and (c) 550 °C. The closed circles and thick lines indicate the number density of the Ga dots and calculated fitting curve. The experimental data were obtained from 14 SREM images at each temperature. The distribution of the data gives a slightly smaller deleted zone width than those obtained in Fig. 5.

$$\Delta G(x) = 16\pi\sigma^3\Omega^2/3\Delta\mu(x)^2, \quad (6)$$

$$\Delta\mu(x) = kT\,\ln[n_s(x)/n_s^e], \quad (7)$$

where N_0, ω, ΔG, σ, Ω, and $\Delta\mu$ are the concentration of adsorption sites, the frequency of atom attachment to critical nucleus, the nucleation barrier, surface-free energy per unit area, the volume of one atom, and the difference in the chemical potential between the adsorbed atom and the atom in the equilibrium state. The surface-free energy of Ga σ is a function of temperature, and is expressed by $[708-0.066(T\text{-}303)]$ $[\mathrm{mJ/m^2}]$.[21] As we mentioned before, in SREM images, the dark area is proportional to the product of the height of a dot and the width of a dot in the horizontal direction. As shown in Fig. 3(a) and Fig. 5, two dots are sometimes superimposed on one another. Hence, in the SREM image, the concentration of the contrast in the horizontal direction might simply not correspond to the number density of a Ga dot. However, in our observation, the number density of Ga dots is small near the linear window, and the size of the dots is nearly uniform. Therefore, the number density of Ga dots $I_n(x)t_d$ can be estimated by using the concentration of contrast in the SREM images shown in Fig. 5. The curves calculated by Eq. (4) were fitted to the concentration by using λ_s and $R_s\tau_{eff}/n_s^e$ as fitting parameters at each temperature. Figure 6 shows a number density of Ga dots $I_n(x)t_d$ as a function of distance x from linear windows in a horizontal direction. Figures 6(a), 6(b), and 6(c) correspond to the deposition temperatures of 450 °C, 530 °C, and 550 °C, respectively. The density is normalized by the saturation value at each temperature at $x=\infty$. The closed circles and thick lines indicate the number density of Ga dots and the fitting curve calculated by Eq. (4). The λ_s and $R_s\tau_{eff}/n_s^e$ found by fitting the curves to the experimental results are summarized in Table I.

The $R_s\tau_{eff}/n_s^e$, the maximum supersaturation ratio, decreases when the substrate temperature is increased. The de-

TABLE I. The λ_s and the $R_s\tau_{eff}/n_s^e$ as a function of the substrate temperature.

T_{sub} (°C)	450	530	550
λ_s (nm)	56.1	70.6	91.7
$R_s\tau_{eff}/n_s^e$	1259.3	107.4	33.3

crease of the supersaturation ratio induces the decrease of the chemical potential difference $\Delta\mu$. This reduces the Ga dot nucleation rate as obtained from Eqs. (4)–(7). This feature coincides with the experimental results in Fig. 5, where the density of Ga dots far from the linear window decreases when the substrate temperature is increased. Since $n_s(x)$ approaches to n_s^e near the window, the depleted zone near the linear windows is mainly produced by the decrease in the Ga dot nucleation rate originating from the decrease of $\Delta\mu$.

The λ_s increases when the substrate temperature is increased. This feature is different from the case where only desorption is considered. The surface-diffusion length determined by desorption (in absence of Ga dots on the surface) decreases when the substrate temperature is increased. On the other hand, the surface-diffusion length determined by the attachment of Ga adatoms to Ga dots (in the absence of desorption) generally increases with the temperature increase due to the decrease in the number density of Ga dots. The surface-diffusion length λ_s in our experiments is thought to be determined by the competition between the desorption rate $(1/\tau_{des})$ and the capture rate by Ga dots $(1/\tau_{nucl})$. That is why the quantitative treatment of the temperature dependence of λ_s is difficult, and this complicated problem is beyond the scope of this paper. Our experiments show that the temperature dependence of $1/\tau_{eff}$ provides a positive temperature dependence of λ_s $(=\sqrt{D_s\tau_{eff}})$. This temperature dependence contributes to the increase in the depleted zone width due to the increase in the substrate temperature. In fact, Eq. (4) and the parameters listed in Table I provide a phenomenological description of our experimental results for the number density of Ga dots in the vicinity of the linear window (Fig. 5).

Ga atoms prefer to form dots on the window rather than on the SiO_2 films. Random dots on SiO_2 films are desorbed easier than well-ordered dots on Si(111) surfaces. Moreover, the λ_s increases when the substrate temperature is increased. Hence, the depleted zone d_z is formed near the Si(111) surface window area, and the width of the depleted zone d_z increases when the substrate temperature is increased. When the width between windows is smaller than $2d_z$, random dots cannot be formed on SiO_2 films. As shown in Fig. 5(c), the width $2d_z$ is about 1 μm at 550 °C. This width is nearly equal to the distance between the windows on which only Ga dots are grown (Fig. 2). These values give important information for the design of periodic windows for selective growth.

IV. SUMMARY

Selective growth of nanometer-scale Gallium dots on patterned ultrathin SiO_2 film was studied by using SREM and EDX. Nanometer-scale Si(111) surface windows were fabricated by the electron-beam-induced thermal decomposition of the film. After that, Ga was deposited on the patterned surfaces at RT-550 °C. We found two processes in which Ga dots grow on Si(111) surface windows only. For the first, Ga was deposited on the patterned surfaces at RT, and then the surface was annealed at 550 °C for more than 5 min. For the second, Ga was deposited at 0.56 ML at a surface temperature of 550 °C. The smallest size of the dots was about 20 nm, and was determined by that of the Si(111) surface window.

To study the mechanism of the selective growth of Ga dots, we measured the desorption rate and the surface-diffusion length of Ga atoms on the SiO_2 surface. The EDX measurement showed that the desorption rate of Ga atoms on SiO_2 films was 2 to 2.5 times larger than that on clean Si(111) surfaces, and that the activation energies of desorption on SiO_2 films was 1.33 eV. The Ga surface-diffusion length was estimated by measuring the temperature dependence of the Ga depleted zone width near the linear Si(111) surface window. The phenomenological nucleation theory was applied to analyze these data. It was found that while the supersaturation ratio decreased when the substrate temperature is increased, the surface-diffusion length increased. The features of desorption, the surface-diffusion length, and the supersaturation ratio explained the mechanism of the selective growth of Ga dots on Si(111) windows.

ACKNOWLEDGMENTS

This paper, partly supported by the New Energy and Industrial Technology Development Organization (NEDO), was performed by the Joint Research Center for Atom Technology (JRCAT) under an agreement between the National Institute for Advanced Interdisciplinary Research (NAIR) and Angstrom Technology Partnership (ATP).

*Permanent address: Institute of Physical Chemistry, Bulgarian Academy of Sciences, 1040 Sofia, Bulgaria.

[1] H. Hirayama, T. Tatsumi, and N. Aizaki, Appl. Phys. Lett. **52**, 2242 (1988).
[2] F. Alexander, D. Zerguine, P. Launay, J. L. Benchimol, and J. Etrillard, J. Cryst. Growth **127**, 221 (1993).
[3] H. Heinecke, A. Brauers, F. Grafharend, C. Plass, N. Puetz, K. Werner, M. Weyers, H. Lueth, and P. Balk, J. Cryst. Growth **77**, 303 (1986).
[4] T. Fukui, H. Saito, M. Kasu, and S. Ando, J. Cryst. Growth **124**, 493 (1992).
[5] K. Hiruma, M. Yazawa, H. Matsumoto, O. Kagaya, M. Miyazaki, and Y. Umemoto, J. Cryst. Growth **124**, 255 (1992).
[6] E. Colas, A. Shahar, B. D. Solle, W. J. Tomlinson, J. R. Hayes, C. Caneau, and R. Bhat, J. Cryst. Growth **107**, 226 (1991).
[7] F. E. Allegetti and T. Nishinaga, J. Cryst. Growth **156**, 1 (1995).
[8] J. H. Neave, P. J. Dobson, B. A. Joyce, and J. Zhang, Appl. Phys. Lett. **47**, 100 (1985).
[9] N. Inoue, J. Cryst. Growth **111**, 75 (1991).
[10] H. Watanabe, K. Fujita, and M. Ichikawa, Surf. Sci. **385**, L952 (1997).
[11] K. Fujita, H. Watanabe, and M. Ichikawa, J. Appl. Phys. **83**, 4091 (1998).

[12] H. Watanabe, K. Fujita, and M. Ichikawa, Appl. Phys. Lett. **72**, 1987 (1998).
[13] S. Fujita, S. Maruno, H. Watanabe, and M. Ichikawa, Appl. Phys. Lett. **69**, 638 (1996).
[14] H. Watanabe, S. Fujita, S. Maruno, K. Fujita, and M. Ichikawa, Jpn. J. Appl. Phys. **36**, 7777 (1997).
[15] A. Shklyaev, M. Shibata, and M. Ichikawa, Appl. Phys. Lett. **72**, 320 (1998).
[16] T. Chikyo and N. Koguchi, Appl. Phys. Lett. **61**, 2431 (1992).
[17] S. Maruno, H. Nakahara, S. Fujita, H. Watanabe, Y. Kusumi, and M. Ichikawa, Rev. Sci. Instrum. **68**, 116 (1997).
[18] M. Ohtsuka and T. Ichikawa, Jpn. J. Appl. Phys. **24**, 1103 (1985).
[19] R. E. Honig and D. A. Kramer, RCA Rev. **30**, 285 (1969).
[20] *Handbook of Crystal Growth*, edited by D. Hurle (North-Holland, Amsterdam, 1993).
[21] S. Hardy, J. Cryst. Growth **71**, 602 (1985).